

## Surface studies of carbon films from pyrolyzed photoresist

R. Kostecki<sup>a</sup>, B. Schnyder<sup>b</sup>, D. Allia<sup>a</sup>, X. Song<sup>a</sup>, K. Kinoshita<sup>a,\*</sup>, R. Kötz<sup>b</sup>

<sup>a</sup>Lawrence Berkeley National Laboratory, Berkeley, CA 94720, USA

<sup>b</sup>Laboratory for Electrochemistry, Paul Scherrer Institut, Villigen PSI CH-5232, Switzerland

Received 7 August 2000; received in revised form 1 May 2001; accepted 29 May 2001

### Abstract

Positive and negative photoresists, which are commonly used in the semiconductor industry, were deposited on silicon wafers by spin coating and then pyrolyzed at temperatures of 600–1100°C in an inert environment to produce thin carbon films. Raman spectroscopy, X-ray photoelectron spectroscopy (XPS) and scanning probe microscopy involving current-sensing atomic force microscopy (CS-AFM) were utilized to characterize the properties of the carbon films. Raman spectroscopy showed two broad bands at approximately 1360 cm<sup>-1</sup> and 1600 cm<sup>-1</sup>, which deconvoluted to four Gaussian bands. The origin of these bands is discussed. CS-AFM showed that the surface conductance increased with increased pyrolysis temperature, and the results are consistent with measurements by a four-point probe method. The XPS spectra revealed the presence of oxygen functional groups (C=O and C–O) on the carbon surface. The relative fraction of oxygen, O/C ratio, decreased as the pyrolysis temperature increased, in agreement with published results. The full-width at half-maximum of the C<sub>1s</sub> peak obtained by XPS also decreased with increasing pyrolysis temperature. © 2001 Elsevier Science B.V. All rights reserved.

**Keywords:** Atomic force microscopy; Carbon; Raman scattering; X-Ray photoelectron spectroscopy

### 1. Introduction

Carbons ranging from bulk commodity carbons (i.e. coke, natural graphite, synthetic graphite) to the more specialty carbons (e.g. carbon aerogels, carbon fibers, mesocarbon microbeads) are available for industrial applications. The morphology and crystallographic properties of these materials vary significantly. For example, highly oriented pyrolytic graphite (HOPG) has a well-ordered surface structure with a significant fraction of basal-plane sites and a small fraction of edge sites. However, high-surface-area amorphous carbon blacks have a surface that consists of predominantly edge sites. More recently, we initiated a project to evaluate thin carbon films for use in microbatteries [1–4]. Pyrolyzing photoresist that was initially spin coated on a silicon wafer produced these carbon films.

A variety of methods such as deposition from plasma [5–9], ion sputtering [10,11], cathodic arc deposition [12,13] and laser evaporation of graphite [14,15] produce carbon films. The term ‘diamond-like’ is often used to describe these carbon films because there is evidence for sp<sup>3</sup> bonding of the carbon atoms in a fourfold structure like diamond. The properties and composition of the carbon films are strongly dependent on the fabrication method, and several reviews are available on these subjects, e.g. by Tsai and Bogy [16], Robertson [17,18], Andersson [19] and Hauser [20]. More recently, Raimondi et al. [21] used laser ablation to carbonize a polyimide to form ring- and cone-like carbon structures.

Our studies showed that the physicochemical properties of the carbon films are strongly dependent on the organic precursor and the processing techniques that are used. Several techniques were used to characterize the surface properties of the carbon films. These include Raman spectroscopy, X-ray photoelectron spectroscopy (XPS) and scanning probe microscopy involving atomic

\* Corresponding author. Tel.: +1-510-486-7389; fax: +1-510-486-4260.

E-mail address: k\_kinoshita@lbl.gov (K. Kinoshita).

force microscopy (AFM). The surface topography of the carbon films was observed on a micro- and nanoscale by AFM. In addition, current-sensing AFM (CS-AFM) was used to probe the surface conductance of the carbon film. The crystallographic structure was ascertained from analysis of the Raman spectra. Information on the surface concentration of oxygen associated with functional groups was derived by XPS. The net result is that a clearer picture of the surface properties of carbon films produced by pyrolyzing photoresist was obtained by combining the information obtained by these techniques, and the results are described in this paper. This study is an extension of our efforts to utilize pyrolyzed photoresist to fabricate microelectrode structures that may be useful in microsensors and microbatteries [1–4].

## 2. Experimental

A detailed description of the preparation of carbon films from photoresist pyrolyzed on silicon wafers was presented elsewhere [2–4]. In brief, a photoresist is spin coated on a silicon wafer (10-cm diameter) that typically has a thin layer of  $\text{Si}_3\text{N}_4$  (thickness of  $\sim 1000$  Å), cured, and then heat treated in an inert atmosphere at temperatures from 600 to 1100°C for 1 h. Two positive photoresists, AZ-4330 (Clariant Corp., Somerville, NJ) and OIR-897 (Arch Chemicals, Norwalk, CT), and a negative photoresist (XPSU, Microchem. Corp., Newton, MA) were used as precursors for producing carbon films. According to the MSDS (Material Safety Data Sheet) information provided by the manufacturers, the positive photoresists are novolak resins, and the negative photoresist is an epoxide resin. For example, the MSDS indicates that the product composition of OIR-897 includes ethyl-3-ethoxypropionate (25–60%), 1-methoxy-2-propanolacetate (15–30%), novolak polymer, reaction products with naphthoquinone diazide ester (12–30%) and novolak polymer (5–15%). No attempt was made to determine the photoresist composition by chemical analysis.

As a typical example, the following procedure was used to produce carbon films. The photoresists were applied manually on the surface of the  $\text{Si}_3\text{N}_4/\text{Si}$  wafer that was spinning at 3000 rev./min. Four applications of positive photoresist were required to produce a layer with a thickness of 8–10  $\mu\text{m}$ . In the case of the negative photoresist, only one application was required to produce a layer of similar thickness. Following spin coating, the wafers were baked at 120°C for 15 min in an ambient environment. Then the wafer was placed in a Lindberg furnace, purged with He, and heated at a rate of 5°C/min to the desired temperature to pyrolyze the photoresist. The pyrolysis temperature was held for 1 h.

Raman spectroscopy measurements were carried out at room temperature in ambient atmosphere using an argon-ion laser (Coherent Inc. Model Innova 70) tuned to 514.5 nm. The resolution of this instrument is approximately  $1.7\text{ cm}^{-1}$ . The Raman spectra were recorded over the spectral region between 1000 and 1800  $\text{cm}^{-1}$ , which provides the most information on the microstructure of carbons. Baseline correction and deconvolution analysis were performed with a commercial software package (PeakFit, version 4.05, SPSS Inc.).

A current-sensing atomic force microscope (Molecular Imaging) with an electronic controller (Park Scientific Instruments) was used to study the surface topography and local electrical conductivity of the carbon film. The AFM was used in the constant-force mode with Pt-Ir coated Si triangular cantilevers (Molecular Imaging) to determine the local conductivity of the carbon surface. These measurements were conducted in a dry nitrogen atmosphere to minimize the effect of a water film on the conductivity.

X-Ray photoelectron spectroscopy (XPS) measurements were performed on an ESCALAB 220i XL (VG Scientific) spectrometer that was equipped with a monochromatic Al X-ray source ( $h\nu = 1486.6\text{ eV}$ ). The measurements were carried out at 200 W power (10 kV, 20 mA) in an analysis chamber at a pressure  $< 5 \times 10^{-9}$  mbar. The Eclipse software package (VG Scientific) was used for data collection and analysis. The XPS measurements were quantified using the cross-sections reported by Scofield [22], the instrumental specific corrections (transmission functions) and the electron escape depth. The instrument was operated at constant analyzer energy mode (CAE-Mode), and the high-resolution spectra were obtained with 20 eV pass energy, which results in a full-width at half maximum (FWHM) of  $< 0.6\text{ eV}$  for Ag  $3d_{5/2}$ . Highly oriented pyrolytic graphite, which is a ZYH-type crystal (Advanced Ceramics Corporation, Lakewood, OH), was used as a reference material.

## 3. Results and discussion

The conversion of the photoresist layer to form a carbon film by heat treatment is accompanied by a significant decrease in thickness. For example, the thickness decreased from  $\sim 8$  to  $\sim 2\text{ }\mu\text{m}$  when the positive photoresist (AZ-4330) was converted to a carbon film at 1000°C. Studies by Madou and co-workers [23] also showed that the shrinkage varied with pyrolysis temperature and gas atmosphere. A significant weight loss (approx. 87%) was observed by thermal gravimetric analysis when the photoresist decomposed during heat treatment [2]. Water, CO,  $\text{CO}_2$ ,  $\text{H}_2$ ,  $\text{CH}_4$  and probably  $\text{N}_2$  are the likely products that form during decomposi

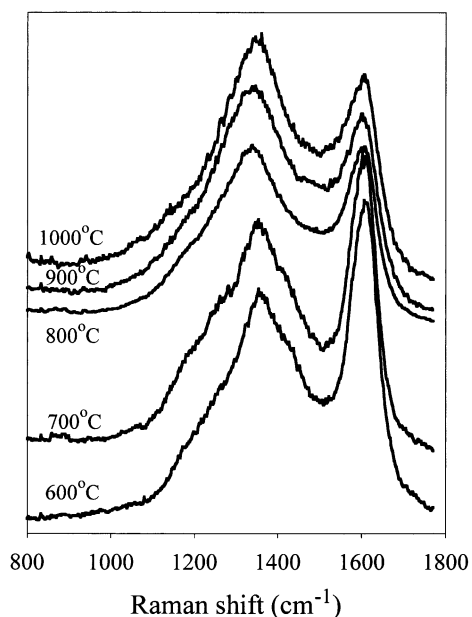


Fig. 1. Raman spectra of pyrolyzed positive photoresist (OIR-897) as a function of pyrolysis temperature.

tion, but these species were not confirmed by chemical analysis. The large shrinkage in thickness of the photoresist to form the carbon film is consistent with the high weight loss.

The methods used in this study to examine the carbon films, Raman spectroscopy, CS-AFM and XPS, are essentially surface-sensitive techniques. By combining these techniques, an array of results were obtained to characterize the surface properties of the carbon films produced by pyrolysis of photoresists. The major focus of this paper will be on the characterization of the carbon film obtained by pyrolyzing positive photoresist OIR-897.

### 3.1. Raman spectroscopy

Raman spectroscopy is a particularly useful tool for characterizing the near-surface structure (i.e. disorder and crystallite formation) of carbon films because carbon is a relatively strong Raman scatterer with two  $E_{2g}$  modes predicted to be Raman active. The strong peak at  $\sim 1582\text{ cm}^{-1}$  in the spectrum of HOPG represents one of the  $E_{2g}$  modes, while the second peak located at  $42\text{ cm}^{-1}$  is difficult to observe.

Raman spectra of carbon films obtained by pyrolysis of the positive photoresist OIR-897 at different temperatures are presented in Fig. 1. Two broad bands are present at approximately  $1360\text{ cm}^{-1}$  and  $1600\text{ cm}^{-1}$ . The relative peak heights change and shift slightly with pyrolysis temperatures. Interestingly, the integrated intensity ratio of 1360/1600 bands increases with the heat-treatment temperature and their positions shift toward lower frequencies, suggesting that the crystal

size decreases with increasing temperature. A similar effect was observed by Sun et al. [24] with carbon films produced by pyrolysis of phenylcarbyne polymer precursor. However, D and G bands broaden, suggesting that the amount of disorder or amorphous phase increases with increasing heat-treatment temperature. Thus the variation of the width and intensity of the D and G bands may suggest that it is related to the growth and size of different carbon phases, presence of functional groups of the precursor material, and adsorbed oxygenated species.

While most authors agree that the peak at  $\sim 1600\text{ cm}^{-1}$  is the first order scattering from the in-plane  $E_{2g}$  mode, the frequency of this peak is given in the literature with noticeable discrepancy depending of the type of carbon and preparation method. Everall et al. [25] demonstrated that laser-induced sample heating can significantly shift the  $E_{2g}$  vibration mode of graphite to lower frequencies. However, the  $E_{2g}$  band broadens and shifts toward higher frequencies with decreasing intraplanar ( $L_a$ ) and interplanar ( $L_c$ ) microcrystallite dimensions. When  $L_a$  and  $L_c$  decrease, a new feature at  $\sim 1360\text{ cm}^{-1}$  is usually observed. This band, which is assigned to the  $A_{1g}$  mode, is associated with the breakage of symmetry occurring at the edges of graphite sheets. Thus, the more edges present, the more phonons that can result in Raman scattering. Other researchers attribute this band to increased disorder in carbon, e.g. in microcrystalline graphite [26]. Tuinstra and Koenig [27] showed that the ratio of  $A_{1g}/E_{2g}$  integrated peak intensities is inversely proportional to the intraplanar microcrystallite distance  $L_a$ .

To resolve the Raman spectra of the carbon films, we applied a standard peak deconvolution procedure after polynomial background subtraction. Fig. 2 shows Raman spectra and fitting results for the samples heat-treated at 700 and  $1000^\circ\text{C}$ . A deconvolution of the Raman spectra of all of the carbon films using a fit with two carbon D and G lines did not give accurate results, thus four Gaussian bands were necessary to account for the observed Raman features with minimum error. Those bands are situated at 1344, 1367, 1591 and  $1622\text{ cm}^{-1}$ . The position of these bands varied very little between samples, however, their intensities changed significantly with pyrolysis temperature. The band at  $1591\text{ cm}^{-1}$  can be assigned to the  $E_{2g}$  graphite mode, and its close neighbor at  $1622\text{ cm}^{-1}$  is typical for 'severely disordered' carbonaceous materials [28]. A very broad, dominant band centered at  $1367\text{ cm}^{-1}$  that extends over the entire spectral range of carbon vibrations is consistent with a disorder-induced peak for highly defective nanocrystalline carbon. Its high intensity and broad bandwidth suggest a significant contribution from various short-order  $sp^2$ - and  $sp^3$ -type carbon structures. The presence of another band at  $1344\text{ cm}^{-1}$  may correspond to the inter-ring stretching mode of aromatic rings of

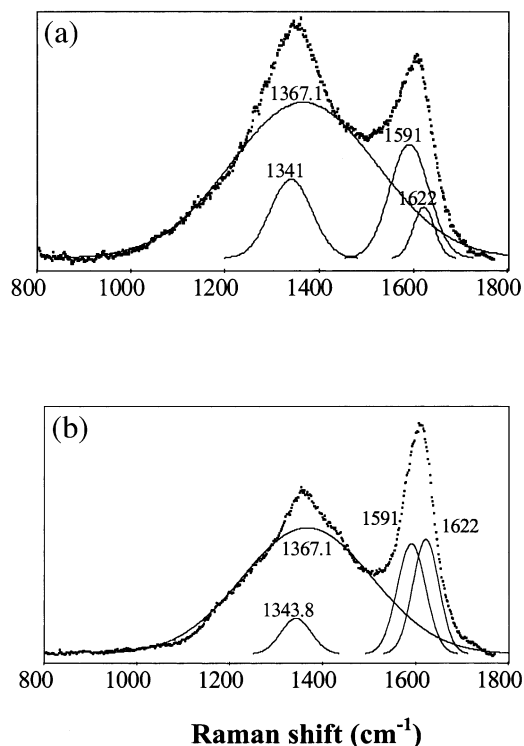


Fig. 2. Four Gaussian deconvolution of the Raman spectra of pyrolyzed positive (OIR-897) photoresist pyrolyzed at 1000°C (a) and 700°C (b).

the original polymer as they are converted into graphitic ribbons and clusters [29].

The relative intensities of the  $E_{2g}$  band and the band at  $1344\text{ cm}^{-1}$  increased with the pyrolysis temperature. Fig. 3 shows the intensity ratio of bands 1591/1622 and 1344/1367 vs. pyrolysis temperature. Both intensity ratios increase steadily between 600 and 800°C and rise abruptly between 800 and 1000°C. The increased intensity of  $E_{2g}$  and  $A_{1g}$  bands with temperature can be interpreted by the advent of larger graphitic crystallites and clusters in the very disordered carbon structure. It is difficult to determine the exact contribution from the  $sp^2$  and  $sp^3$  structures in the quantitative manner. Both structure fractions can contribute to 'the amorphous-carbon' band at  $1367\text{ cm}^{-1}$  because of the different Raman cross-section of  $sp^2$  and  $sp^3$  carbon sites. On the other hand, carbon oxygen bonds, e.g.  $-C-O-$ ,  $-C=O$ , can generate Raman bands approximately 1350 and  $1600\text{ cm}^{-1}$ , respectively.

For flat surfaces containing an adsorbed monolayer, it is clear that even with an optimized system the Raman signal from the surface species will be very difficult to detect without an enhancement mechanism of the Raman scattering. However, with a surface consisting of a large number of nanocrystallites, a large fraction of grain boundaries is present as sites for adsorbed species. The bands at 1622 and  $1367\text{ cm}^{-1}$  in the Raman spectra of

pyrolyzed photoresist suggests that adsorbed surface species, most likely oxygenated carbon groups, may be detectable with normal Raman spectroscopy. The sampling depth for carbon is approximately 30 nm with Raman spectroscopy, which is approximately 10 times larger than that for XPS, when visible light is used. This sampling depth is sufficient to probe microstructural changes near the carbon surface as well as to collect the signal from the adsorbed species from within this light penetration range.

### 3.2. Current-sensing atomic force microscopy

AFM studies [30,31] of carbon films derived from pyrolyzed positive photoresists (AZ-4330 and OIR-897) clearly showed that an atomically smooth surface is obtained from a pyrolyzed photoresist. The AFM images of the carbon films revealed a compact surface structure that appears to be relatively smooth, uniform and free of cracks and large aggregates. This structure is typical of the carbon films obtained by pyrolysis at 700–1000°C in an inert atmosphere. Statistical analysis of this featureless surface revealed a peak-to-valley distance of  $\sim 10\text{ Å}$  and root-mean-square (r.m.s.) roughness of  $\sim 2\text{ Å}$  over an area of  $0.5\text{ }\mu\text{m} \times 0.5\text{ }\mu\text{m}$ .

Current-sensing AFM was used to measure the topography and surface conductance of the carbon films in a dry nitrogen atmosphere. The result observed with a carbon film that was obtained from a positive photoresist

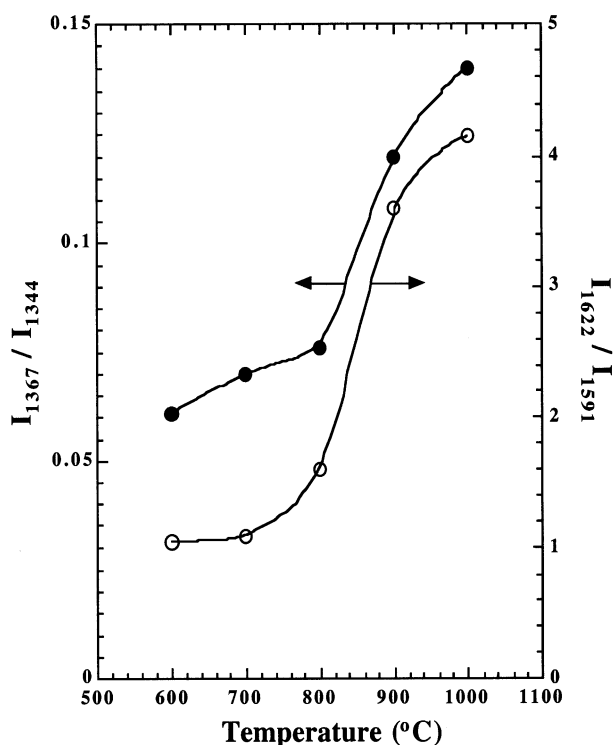


Fig. 3. Raman intensities ratio of  $I_{1591}/I_{1622}$  and  $I_{1343}/I_{1367}$  as a function of pyrolysis temperature.

(OIR-897 pyrolyzed at 1000°C) is shown in Fig. 4. The dark and light regions represent areas of high conductance and low conductance, respectively. The surface of the carbon film appears to have a relatively homogeneous conductance and an atomically smooth surface, as noted above. At a bias of +0.05 V, there is a clear match between the high regions in the topography map and low conductivity. The carbon films obtained from the positive photoresist (OIR-897) had higher surface conductance than carbon films obtained from the negative photoresist (XPSU). Although we do not present the data, a comparison of the surface resistance (reciprocal of surface conductance) obtained by CS-AFM and the sheet resistance from four-point probe measurements show a similar trend with pyrolysis temperature. The results showed that a high sheet resistance was observed with carbon films produced at low pyrolysis temperatures (i.e. <700°C). The sheet resistance measured for a carbon film produced by pyrolysis at 600°C was close to 100 000 ohm/□. The corresponding sheet resistance for a carbon film produced at 1000°C was approximately 10 ohm/□. After pyrolysis at temperatures above 700°C, the resistance decreased dramatically, which is believed to be due to changes in the film composition (e.g. decreasing H/C ratio) as the pyrolysis temperature increased [32–34].

### 3.3. X-Ray photoelectron spectroscopy

The XPS data for the positive photoresist OIR-897, which was pyrolyzed at different temperatures, were analyzed to determine the atomic concentration ratio O/C from the C<sub>1s</sub> and O<sub>1s</sub> spectra. Examples of the

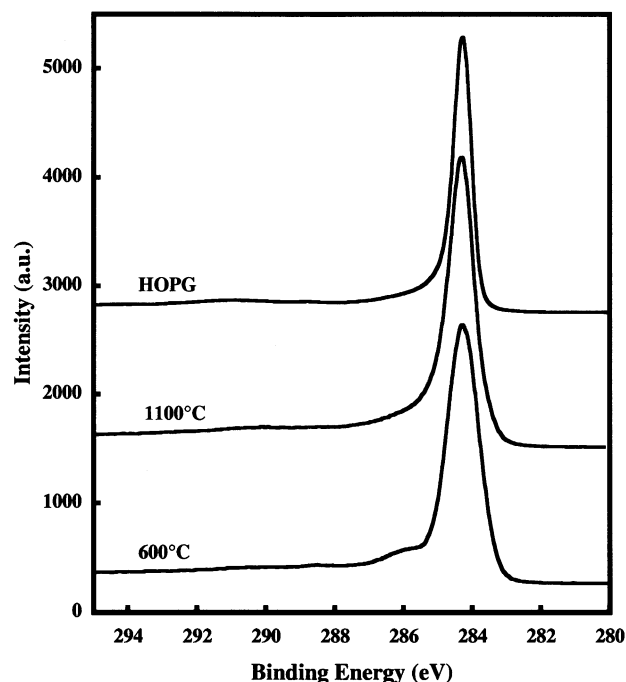


Fig. 5. XPS spectra for the C<sub>1s</sub> peak obtained with HOPG and a photoresist (OIR-897) that was pyrolyzed at 600°C and 1000°C.

XPS spectra for the C<sub>1s</sub> peak obtained with HOPG and a photoresist that was pyrolyzed at 600 and 1000°C are shown in Fig. 5 for binding energies in the range 280–290 eV. The spectra are all typical of the C<sub>1s</sub> peak observed with other carbon [35]. The peaks have an asymmetric shape with a long tail component present at higher binding energies. Takahagi and Ishitani [35]

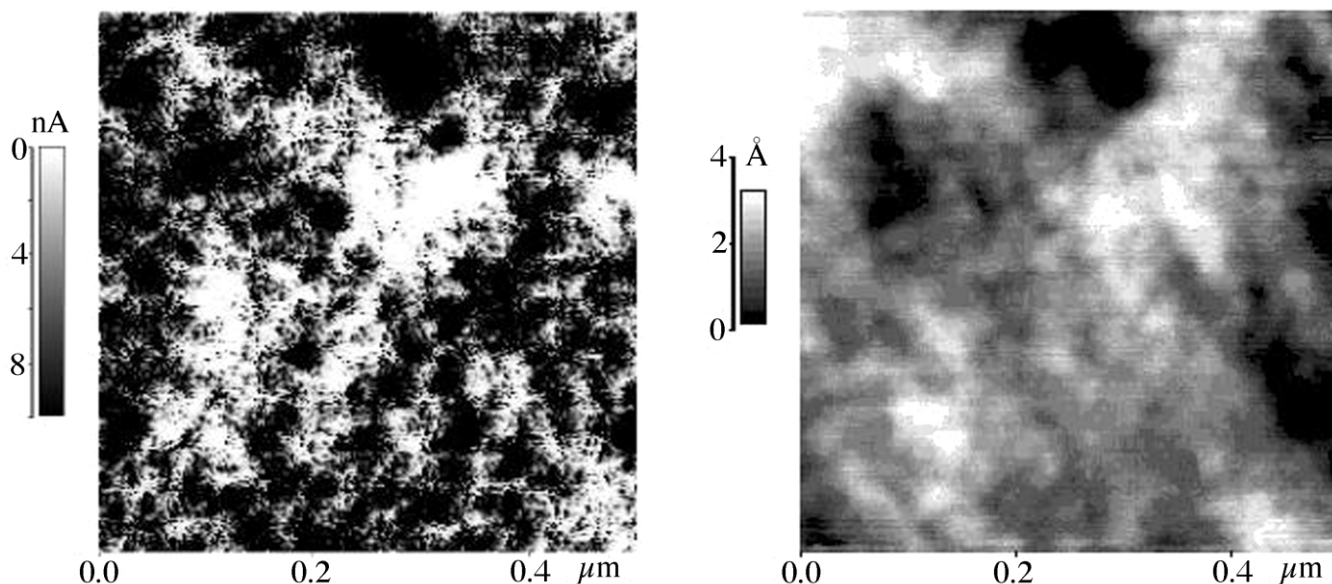


Fig. 4. Topography (right) and surface conductance (left) of carbon film obtained by pyrolysis of positive photoresist (OIR-897) at 1000°C. Surface conductance obtained by CS-AFM. Bias of +0.05 V.

observed a clear trend between the XPS  $C_{1s}$  spectra and the Raman spectra in the range  $1250\text{--}1650\text{ cm}^{-1}$  for carbon fibers. The peaks in the respective spectra became narrower with an increase in the heat-treatment temperature of the carbon fiber. Furthermore, the peak at  $1360\text{ cm}^{-1}$  in the Raman spectra decreased in intensity with increased heat-treatment temperature. This latter observation is not consistent with the Raman spectra shown in Fig. 1 for pyrolyzed photoresist. However, it should be noted that our carbon films were produced at much lower temperatures, i.e.  $\leq 1000^\circ\text{C}$ , than the heat-treatment temperatures ( $1350\text{--}2500^\circ\text{C}$ ) used by Takahagi and Ishitani [35].

The FWHM was determined from the  $C_{1s}$  spectra and the results are presented in Fig. 6. For freshly cleaved HOPG, the FWHM is  $0.62\text{ eV}$ . However, the FWHM for the carbon films obtained from pyrolyzed photoresist is much higher, and the values decreased with an increase in pyrolysis temperature. According to Barr and Seal [36], the narrow peak width of graphite is due to its high conductivity and the large crystalline structure, in agreement with the conclusions of Takahagi and Ishitani [34]. Pyrolyzed carbon films have a much smaller crystallite size; consequently their XPS spectra show a broader FWHM. Furthermore, these carbon films are less conductive than HOPG. The decrease in FWHM of pyrolyzed photoresist with increasing pyrolysis temperature indicates an increase in conductivity. A similar decrease was observed [37] in the FWHM of coke that was calcined at different temperatures. These findings are consistent with an increase in the surface conductance of the pyrolyzed photoresist that was observed by CS-AFM. From these results, we conclude that the FWHM of the  $C_{1s}$  spectra of carbonaceous material can

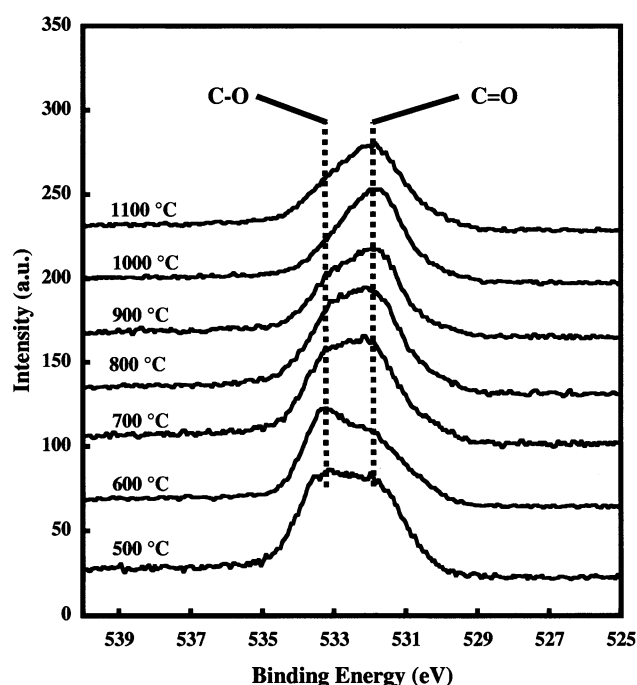


Fig. 7. XPS spectra of the  $O_{1s}$  peak obtained with a positive photoresist (OIR-897) that was pyrolyzed at  $500\text{--}1000^\circ\text{C}$ .

be interpreted as a measure of the crystallite size and surface conductivity.

The XPS  $O_{1s}$  spectra for the carbon films obtained from pyrolyzed photoresist (OIR-897) are presented in Fig. 7 for binding energies in the range  $525\text{--}540\text{ eV}$ . Analysis of the spectra suggests that two different oxygen species with peak positions at  $531.9$  and  $533.1\text{ eV}$  are present on the carbon surface. According to Jimenez Mateos [37], the peak at  $533.1\text{ eV}$  can be

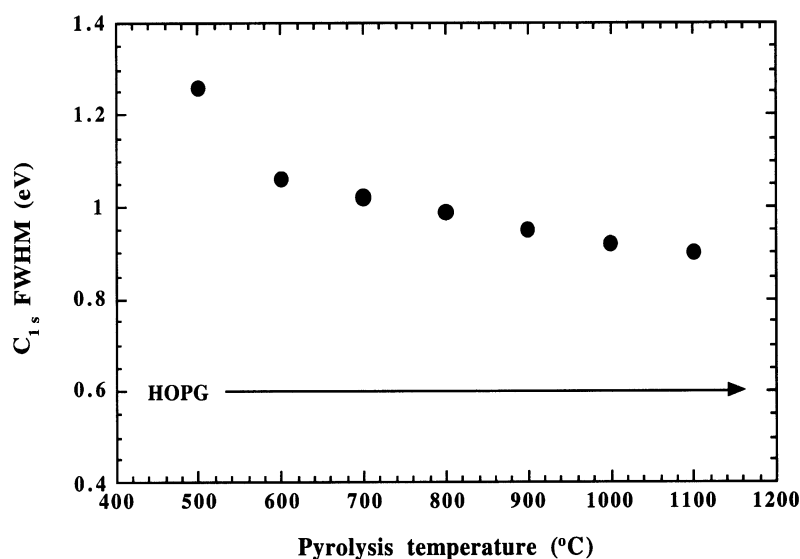


Fig. 6. Variation in FWHM for  $C_{1s}$  peak with pyrolysis temperature of positive photoresist (OIR-897).

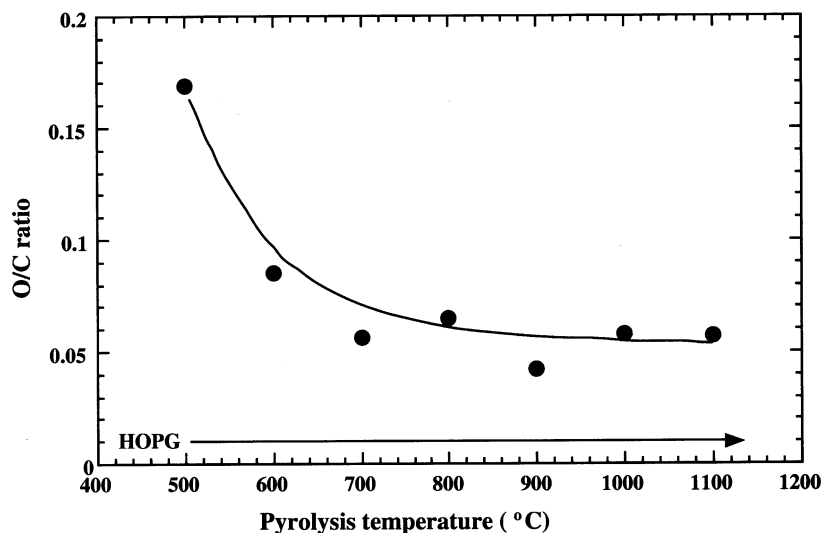


Fig. 8. Dependence of oxygen content (O/C) on the pyrolysis temperature of positive photoresist (OIR-897).

assigned to C–O and the one at 531.9 eV to C=O. These peak assignments agree with those suggested by Xie and Sherwood [38] who indicated that the peak at ~533.9 eV originates from C–OH, and the one at ~531.1 eV is due to C=O and/or C–O–C. Inspection of the XPS spectra in Fig. 7 shows a noticeable change in the peak profiles with pyrolysis temperature. There is no evidence in the XPS spectra for adsorbed water or chemisorbed oxygen, which is indicated by a peak at ~535.5 eV [38]. The carbon film obtained at 500°C shows qualitatively two overlapping peaks that are close to equal intensity. As the pyrolysis temperature increases, the peak profile changes with an increase in the C=O peak and a diminution of the C–O peak. The O/C ratio is essentially constant at higher pyrolysis temperatures (see discussion below), therefore this result implies that the C=O surface species increases whereas the amount of C–O species decreases.

Because the carbon films were stored in the laboratory ambient environment, this exposure to air can lead to gradual oxidation of the surface. Ranganathan et al. [23] observed a slow increase in the O/C ratio of carbon films produced from pyrolyzed positive photoresist that was exposed to air. The formation of oxygen groups on the carbon film by reaction to oxygen in air cannot be disregarded, however, the trend of the XPS data suggests that the pyrolysis temperature have a stronger influence on the O/C ratio. Jenkins and Kawamura [39] investigated the carbonization of polymers by heat treatment and observed four temperature ranges for the pyrolysis reactions. The polymer turns black during low-temperature (typically <300°C) heat treatment in the pre-carbonization stage. The temperature range between 300 and 500°C is the carbonization stage where oxygen, nitrogen, etc., are removed. This is followed by the

gradual elimination of hydrogen in the dehydrogenation stage between 500 and 1200°C. Finally, the annealing stage occurs above 1200°C. From these observations, it appears that pyrolysis temperatures >500°C are required to eliminate most of the oxygen in the polymer.

The oxygen content (O/C) of the pyrolyzed photoresist (OIR-897) was determined from the  $C_{1s}$  and  $O_{1s}$  spectra. These values are plotted as a function of the pyrolysis temperature in Fig. 8. The O/C ratio decreases gradually with an increase in the pyrolysis temperature and reaches a limiting value of approximately 0.05 at temperatures >700°C. In contrast, the O/C ratio for HOPG is considerably lower, approximately 0.01. The decrease in oxygen content with increasing heat-treatment temperature is consistent with the XPS results observed with other carbons. Carbon-oxygen surface complexes (i.e. C–O, C=O) desorb from the carbon surface at elevated temperatures [40–42], consequently the O/C ratio is expected to decrease with an increase in pyrolysis temperature of the photoresist.

#### 4. Concluding remarks

Raman spectroscopy, atomic force microscopy and X-ray photoelectron spectroscopy were used to investigate carbon films obtained by pyrolysis of positive or negative photoresists. The physicochemical properties of these carbon films changed as a function of the pyrolysis temperature in the range from 600 to 1000°C. A deconvolution of the Raman spectra of the carbon films using four Gaussian bands situated at 1344, 1367, 1591 and 1622  $\text{cm}^{-1}$  provided the best fit to the data. The Raman spectra of the carbon films are consistent with a highly defective nanocrystalline carbon with a significant contribution from various short-order  $\text{sp}^2$ - and  $\text{sp}^3$ -type

carbon and aromatic rings of the original structure of the polymer. Current-sensing AFM and four-point probe measurements revealed that the carbon films produced at a low pyrolysis temperature (600°C) have high resistance, but it decreased dramatically for carbon films obtained at a temperature of 1000°C. The AFM analysis also showed that atomically smooth carbon films are obtained by pyrolysis of the photoresists. The XPS O<sub>1s</sub> spectra of the carbon films obtained from positive photoresist OIR-897 suggest that two different oxygen species with peak positions at 531.9 and 533.1 eV are present, which can be assigned to C=O and/or C–O–C and C–OH, respectively. As the pyrolysis temperature increases, the peak profiles change with an increase in the C=O peak and a decrease in the C–O peak. The oxygen content (O/C) of the pyrolyzed photoresist decreases gradually with an increase in the pyrolysis temperature and reaches a limiting value of approximately 0.05 at temperatures >700°C. The decrease in the carbon–oxygen surface complexes (i.e. C–O, C=O) content with increasing heat-treatment temperature is also consistent with the Raman data.

## Acknowledgements

Financial support by the Office of Energy Research, Office of Basic Energy Sciences, Chemical Sciences Division of the U.S. Department of Energy, contract No. DE-AC03-76SF00098 and the Swiss National Science Foundation, Grant No. 4036-044040, are gratefully acknowledged.

## References

- [1] M. Madou, A. Lal, G. Schmidt, X. Song, K. Kinoshita, M. Fendorf, A. Zettl., R. White, Carbon micromachining (C-MEMS), in: A. Ricco, M. Butler, P. Vanysek, G. Horvai, A. Silva (Eds.), Proceedings of the Symposium on Chemical and Biological Sensors and Analytical Electrochemical Methods, 97-19, The Electrochemical Society, Inc, Pennington, NJ, 1997, p. 61.
- [2] J. Kim, X. Song, K. Kinoshita, M. Madou, R. White, J. Electrochem. Soc. 145 (1998) 2314.
- [3] R. Kostecki, X. Song, K. Kinoshita, Electrochem. Solid Stat. Lett. 2 (1999) 461.
- [4] K. Kinoshita, X. Song, J. Kim, M. Inaba, J. Power Sources 81 /82 (1999) 170.
- [5] M.A. Tamor, W. Vassell, K. Carduner, Appl. Phys. Lett. 58 (1991) 592.
- [6] H. Windischmann, G. Epps, J. Appl. Phys. 68 (1990) 5665.
- [7] H. Windischmann, G. Epps, J. Appl. Phys. 69 (1991) 2231.
- [8] M. Yoshikawa, G. Katagiri, H. Ishida, A. Ishitani, M. Ono, K. Matsumura, Appl. Phys. Lett. 55 (1989) 2608.
- [9] M.A. Tamor, J. Haire, C. Wu, K. Hass, Appl. Phys. Lett. 54 (1989) 123.
- [10] M. Yoshikawa, G. Katagiri, H. Ishida, A. Ishitani, T. Akamatsu, Appl. Phys. Lett. 52 (1988) 1639.
- [11] J. Cuomo, D. Pappas, J. Bruley, J. Doyle, K. Saenger, J. Appl. Phys. 70 (1991) 1706.
- [12] R. Lossy, D. Pappas, R. Roy, J. Doyle, J. Cuomo, J. Bruley, J. Appl. Phys. 77 (1995) 4750.
- [13] R. Lossy, D. Pappas, R. Roy, J. Doyle, J. Cuomo, V. Sura, Appl. Phys. Lett. 61 (1992) 171.
- [14] D. Pappas, K. Saenger, J. Bruley, W. Krakow, J. Cuomo, J. Appl. Phys. 71 (1992) 5675.
- [15] D. Pappas, K. Saenger, J. Cuomo, R. Dreyfus, J. Appl. Phys. 72 (1992) 3966.
- [16] H. Tsai, D. Bogy, J. Vac. Sci. Technol. A 5 (1987) 3287.
- [17] J. Robertson, Adv. Phys. 35 (1986) 317.
- [18] J. Robertson, Prog. Solid Stat. Chem. 21 (1991) 199.
- [19] L. Andersson, Thin Solid Films 86 (1981) 193.
- [20] J. Hauser, J. Non-Cryst. Solids 23 (1977) 21.
- [21] F. Raimondi, S. Abolhassani, R. Brüttsch, F. Geiger, T. Lippert, J. Wambach, J. Wei, A. Wokaun, J. Appl. Phys. 88 (2000) 3659.
- [22] J.H. Scofield, J. Electron Spect. Relat. Phenom. 8 (1976) 129.
- [23] S. Ranganathan, R. McCreery, S.M. Majji, M. Madou, J. Electrochem. Soc. 147 (2000) 277.
- [24] Z. Sun, X. Shi, X. Wang, Y. Sun, Diamond Relat. Mater. 8 (1999) 1107.
- [25] N.J. Everall, J. Lumsdon, D.J. Christopher, Carbon 29 (1991) 133.
- [26] R. Vidano, D.B. Fischbach, J. Am. Ceram. Soc. 61 (1978) 13.
- [27] F. Tuinstra, J.L. Koenig, J. Phys. Chem. 53 (1970) 1126.
- [28] M. Nakamizo, K. Tamai, Carbon 22 (1984) 197.
- [29] M.J. Matthews, X.X. Bi, M.S. Dresselhaus, Appl. Phys. Lett. 68 (1996) 1078.
- [30] R. Kostecki, X.Y. Song, K. Kinoshita, J. Electrochem. Soc. 147 (2000) 1879.
- [31] D. Allia, R. Kostecki, X. Song, K. Kinoshita, R. Kötz, 11th International Meeting on Lithium Batteries, May 28–June 2, 2000, Como, Italy, 2000.
- [32] H.Q. Xiang, S.B. Fang, Y.Y. Jiang, J. Electrochem. Soc. 144 (1997) L187.
- [33] T. Zheng, Q. Zhong, J. Dahn, J. Electrochem. Soc. 142 (1995) L211.
- [34] T. Zheng, Y. Liu, E. Fuller, S. Tseng, U. von Sacken, J. Dahn, J. Electrochem. Soc. 142 (1995) 2581.
- [35] T. Takahagi, A. Ishitani, Carbon 26 (1988) 2581.
- [36] T.L. Barr, S. Seal, J. Vac. Sci. Technol. A 13 (1995) 1239.
- [37] J.M. Jimenez Mateos, J.L. Fierro, Surf. Interface Anal. 24 (1996) 223.
- [38] Y. Xie, P. Sherwood, Chem. Mater. 1 (1989) 427.
- [39] G.M. Jenkins, K. Kawamura, Polymeric Carbons — Carbon Fibre, Glass and Char, Cambridge University Press, Cambridge, UK, 1976.
- [40] E. Papirer, J. Dentzer, S. Li, J. Donnet, Carbon 29 (1991) 69.
- [41] S. Barton, D. Gillespie, B. Harrison, Carbon 11 (1973) 649.
- [42] M. Coltharp, N. Hackerman, J. Phys. Chem. 72 (1968) 1171.